

Nature of the dead layer in CdS and its effect on exciton reflectance spectra

F. Evangelisti,*† A. Frova,† and F. Patella

Istituto di Fisica dell'Università di Roma, Rome, Italy

(Received 10 June 1974)

Experimental spectra of exciton reflectance in CdS at $\sim 2^\circ\text{K}$ are measured for different conditions of the surface. The results are explained in terms of optical interference across a "dead layer" which can be of either intrinsic or extrinsic origin. In the former case, a one-to-one correspondence between the dead-layer depth and the orbital size of each hydrogenic line is established. The Hopfield and Thomas additional boundary conditions with spatial dispersion are shown to be quite adequate at explaining the observed features. The general significance of the surface interference effect in the reflectance behavior of Wannier excitons is demonstrated by consideration of results known for other semiconductors.

I. INTRODUCTION

In order to explain certain deviations from classical oscillator reflectance, observed in exciton spectra of cadmium sulphide, Hopfield and Thomas were first to invoke spatial dispersion effects, i.e., wave-vector dependence of the optical dielectric functions. In this case, one deals with two waves propagating in the medium; a single-valued solution for the reflectance can no longer be derived from Maxwell's equations unless an appropriate boundary condition is additionally introduced. This may be selected, for instance, in a way that specifies the physical behavior of the exciton near the surface. The problem has been investigated by various authors;¹⁻⁶ the condition which is most frequently used is to assume that the exciton polarization be zero at the surface^{1,2} or at some depth l from the surface.¹ The latter choice, that should apply better to the case of large-sized Wannier excitons, implies a surface region where no excitons can be created, the "dead layer." The calculated reflectance line shape is critically dependent on the additional boundary condition chosen; moreover, in the dead-layer case, surface interference effects are to be expected. As a matter of fact, experimental reflectance spectra of a number of semiconductors, such as PbI_2 ⁷ and GaAs ,⁸ can be interpreted in terms of spatial dispersion only if allowance for an exciton-free surface layer is made. Similar conclusions are reached by investigation of the phase shift upon reflection in CdS ⁹ and ZnO .⁹

On the other hand, in a study of some III-V compounds, i.e., GaAs and InP ,¹⁰ it has been conclusively shown that the application of an external electric field, normal to the reflecting surface, can drastically alter the line shape of the ground-exciton reflectance, which can be fully turned upside down by a suitable choice of the applied voltage. This was explained in terms of a surface op-

tical-interference effect due to the creation of an extended surface dead layer caused by field-induced ionization of the exciton. The data suggested that the strong spectral alterations observed are only weakly dependent on spatial dispersion effects and on the detailed physical nature of the dead layer.

The above arguments underscore the importance of a thorough investigation of the surface region; this should provide a better understanding of the role of spatial dispersion and boundary conditions in connection with many unexplained features of exciton reflectance spectra. For instance, it is well known that strong line-shape differences are found among different materials and, in a given material, among the various levels of the hydrogenlike excitonic series. Quite often, even a given line may look rather different from sample to sample of the same semiconductor; the $n=2$ and higher excited levels, for example, are usually detected only in samples which can be said to have a "good" surface. This is the case of CdS, a material of special interest because of its large longitudinal-transverse exciton splitting, which should make the effect of spatial dispersion particularly evident. On the other hand, CdS exhibits many interesting surface-dependent effects, as shown by its photoconductivity,^{11,12} luminescence,¹³ and surface-photovoltage behavior.¹⁴ We may therefore count on the possibility of altering the "quality" of the surface in a number of known ways.

The aim of the present work is to elucidate the details of the boundary conditions, as discussed above, by a line-shape analysis of the reflectance spectra of the three lowest-lying levels of the A exciton in CdS. The material is first investigated in as-grown form and then again after the surface conditions are varied by heat treatments in vacuum or in a suitable atmosphere. In Sec. II we shall briefly outline the state of knowledge of the equilibrium surface configuration of virgin and moderately treated CdS crystals. The correspond-

ing experimental spectra will be given in Sec. III A, along with an interpretation of their behavior in terms of surface interference. A one-to-one correspondence between line shape and exciton average size will be established for the three levels of CdS under investigation and also for other materials previously studied. Section III B is devoted to results obtained in heavily treated samples where a very extended dead layer has been intentionally created. It will be shown that this type of data lends further support to the validity of Thomas and Hopfield's additional boundary conditions, which are at the basis of the dead-layer picture. Conclusions will be drawn in Sec. IV, where it will be recalled that the picture derived from the present investigation is the only one capable of explaining all the features of CdS exciton spectra, ruling out, for instance, models calling for a splitting of the exciton levels.

II. SURFACE LAYER OF CdS

It is well known that as-grown CdS platelets are usually classified as belonging to class I or class II,¹⁵ according to whether liquid-nitrogen photoconductivity shows a peak or a dip at the $n=1$ exciton energy. The difference seems to be related to the type of surface field^{16,17} which, in class II, favors the surface recombination process in various ways. An analysis of this behavior has been recently carried out by Boer and co-workers,^{18,19} who propose two surface band structures for CdS, depending on whether the surface does or does not contain a nonstoichiometric excess of Cd ions acting as shallow donors. Cd-rich layers are a result of the growth method and cause class I behavior. For compensated CdS, the two possible equilibrium band schemes are shown in Fig. 1; at the low temperature of interest in our experiment, one has to deal in all cases with depletion layers, as illustrated by the field profiles given at the top. It is assumed for simplicity that in part (a) of the figure the Cd-excess donors are evenly distributed in the nonstoichiometric layer. If its thickness is much smaller than the underlying depletion region, the latter is the critical region and the crystal has, respectively, class I or class II behavior depending on which charge is dominant, i.e., the Cd donors or the surface-state acceptors. Surface states in CdS are essentially related to chemisorbed oxygen. As their presence is strictly a function of the partial oxygen pressure in the ambient, samples without a Cd-rich layer in vacuum are likely to have little or no surface field. Transition from configuration (a) to (b) in Fig. 1 can be achieved by moderate heating in a vacuum, a process which causes

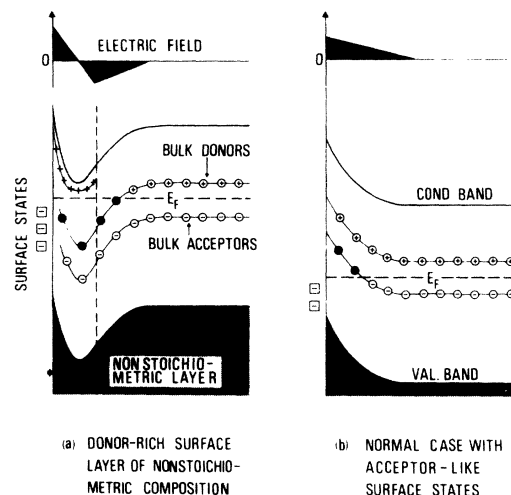


FIG. 1. Surface energy-band configuration of compensated CdS with (a) and without (b) a layer of excess Cd donors. The electric field profile is shown at the top.

evaporation of excess Cd.¹⁹ Further heating produces evaporation of both Cd and S with creation of a new layer of nonstoichiometric composition and a certain amount of deterioration in the quality of the surface. This treatment, however, may not give rise to a controllable reversal from Fig. 1(b), class II behavior, to Fig. 1(a), class I behavior. In the following, we shall take advantage of the above-mentioned temperature effects to vary the surface dead layer over a wide range of thicknesses.

III. EXPERIMENTAL RESULTS AND DISCUSSION

A. Virgin and moderately treated crystals

The investigation was performed on a number of high-resistivity compensated CdS samples, all grown by the vapor-transport method, but obtained from two different sources. Samples labeled B were supplied by the University of Delaware, the others by General Motors, Inc. In all cases, normal-incidence reflectance was measured from a plane containing the c axis for light polarized both parallel and perpendicular to it. Since we intend to apply our discussion to the A exciton, which is not seen in the parallel case, only data for perpendicular polarization will be presented. All measurements were made with samples immersed in superfluid helium ($\sim 2^\circ\text{K}$). Prior to cooling, the sample chamber was evacuated to 10^{-3} Torr for about 30 min. This probably resulted in the elimination of a large fraction of the surface states due to oxygen. The absolute value of the reflectance often varied from sample to sample and, to a much smaller extent,

for different positions of the light spot on one and the same sample. This was attributed to the presence of steps, microscopic cracks, or other physical damage on the surface. All spectra to be shown have therefore been renormalized to give, for the reflectance at 4890 Å, the same value of 0.31 as observed in one case.

Spectra for virgin as-grown crystals are given by the curves of Fig. 2 and by the top curve of Fig. 3. One observes two characteristic features which are consistently found in all samples. The line shape of the $n=1$ structure, both for the A and B exciton, is always different from that of the $n=2$ level. The former exhibits a peak followed by a valley, while in the latter the sequence is reversed. This behavior is not peculiar of CdS, as it is found in other II-VI compounds showing the $n=2$ structure (e.g., ZnSe²⁰ and CdSe²¹). The $n=3$ level is detected only in a moderately treated sample (see later for details) and is shown in the box of Fig. 3. Its line shape is still different, having the form of a dip. The main discrepancy among the various samples, in reference to the $n=1$ level, is found at the longitudinal frequency ω_L , where the characteristic "spike," first reported by Hopfield and Thomas,¹ sometimes is present and sometimes is not. This may be related to some extent to a variation of the damping, but we shall demonstrate in the following that it is more reasonably attributed to differences in the dead-layer depth. This connection will actually entirely account for the line-shape behavior and, in particular, for the discrepancies among the various levels. It will also explain another important feature in the experimental data, i.e., the uneven amplitude of the $n=2$ structure. Note that samples with a clear $n=2$ structure may have no spike or vice versa, a result which stresses the inadequacy of a description in terms of damping differences.

Let us consider the Hopfield and Thomas additional boundary conditions,¹ whereby the exciton contribution to the polarizability is set equal to zero over a finite volume. The physical origin of this layer is obviously related to the impossibility for the exciton to have its center of mass closer to the surface than the exciton radius itself, without being severely distorted. Thus, the magnitude of the dead layer can be quite appreciable for Wannier-type excitons, whose Bohr radius can vary from tens (II-VI semiconductors) to hundreds of angstroms (III-V semiconductors). Let us examine Fig. 4 where we have reported the binding energy of the fundamental exciton level as a function of the distance Z of its center of mass from the surface. The curve has been calculated by Deigen and Glinchuk²² by consider-

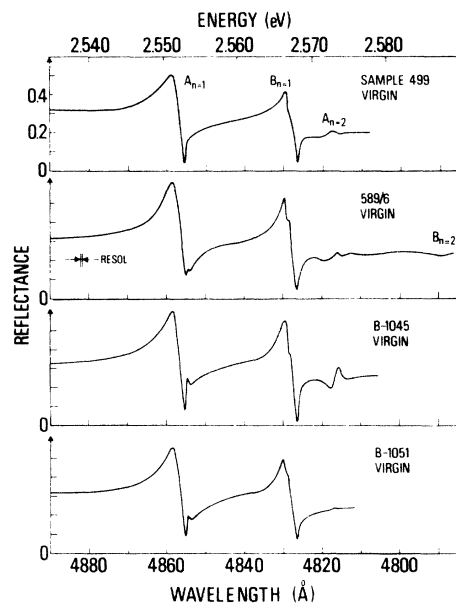


FIG. 2. Experimental normal-incidence reflectance of various as-grown CdS platelets. The light vector is polarized perpendicular to the c axis. All curves are normalized to have the same value at 4890 Å.

ing the influence of the image forces on both the electron and the hole approaching the surface. The exciton binding energy is found to equal the bulk effective Rydberg only far away from the surface. For $Z \sim 1.5$ Bohr radii, ionization occurs.

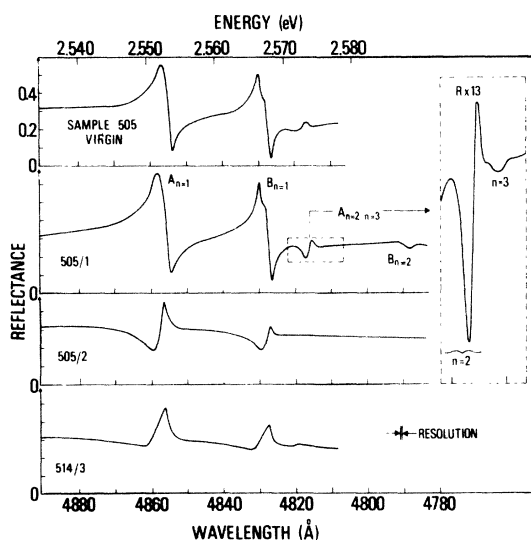


FIG. 3. Experimental normal-incidence reflectance of CdS platelets. Conditions are the same as in Fig. 7 except: second curve from top, sample 505 treated at 790 °C; third curve from top, sample 505 treated at 940 °C; bottom curve, sample 514 treated at 800 °C (see text for details).

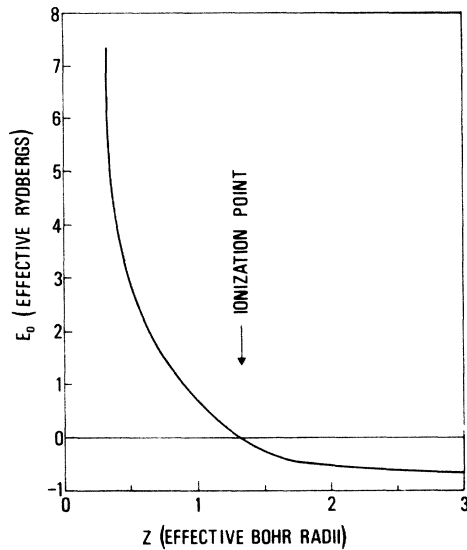


FIG. 4. Exciton binding energy in effective rydberg units as a function of the distance from the surface of the exciton center of mass (measured in effective Bohr radii).

Correspondingly, one should have a layer where the exciton polarizability is gradually decreasing from its bulk value to zero. The dead layer we have so depicted is clearly of intrinsic origin and bears no connection with the particular conditions of the surface, taken as an ideal geometric boundary. In general, there will be other contributions to the dead layer, as we shall see in the course of our discussion. Whatever the origin of the dead layer may be, we are able to discuss its effect on the reflectance in terms of interference between the light beams reflected at the vacuum-semiconductor and at the dead-layer-bulk boundaries. This effect is present independently of the magnitude of the spatial dispersion effect; the line shape is primarily determined by the phase delay between the two interfering beams and to a weaker extent by spatial dispersion. This has been demonstrated for GaAs and InP in earlier publications.^{10,23} Calling l the dead-layer depth and λ_m the light wavelength in the semiconductor, the round-trip phase delay is

$$\theta = 4\pi l / \lambda_m, \quad (1)$$

i.e., directly proportional to l . Consistent with its physical origin, l must be correlated with the exciton size, increasing along with the n number of the level considered. Lacking a quantitative calculation which takes into account exactly the exciton confinement effect due to the surface, the dead-layer depth is not sharply defined. We assume therefore as a reference parameter the

average exciton diameter, equal to

$$\langle d \rangle = 3n^2 r_B \quad (2)$$

(r_B is the exciton Bohr radius). We now calculate the line shape of the normal-incidence reflectance of the three lowest levels of the A exciton in CdS, using the phase angle θ as a parameter. We shall then compare with experiment to establish a correspondence between $\langle d \rangle$ in Eq. (2) and l in Eq. (1) giving best agreement. The results of the calculation are shown in Figs. 5–7 for a choice of θ 's. We have assumed that, in the absence of perturbation, the contribution to the dielectric function of every excitonic line ω_{0n} is given by a term of the type

$$\epsilon_n = \frac{1}{n^3} \frac{4\pi\alpha\omega_{0n}^2}{\omega_{0n}^2 - \omega^2 + \hbar K^2 \omega_{0n} / M^* - i\omega\Gamma}. \quad (3)$$

In Eq. (3), $4\pi\alpha$ is the exciton polarizability, K and M^* are, respectively, the total exciton wave vector and mass, and Γ is an appropriate broadening parameter. The K -dependent term accounts for spatial dispersion. It should be emphasized that the dead layer is a region of strong inhomogeneity (see Fig. 4), a feature which we cannot duly include in the calculations. We resort then to the uniform-layer approximation in the spirit of the Hopfield and Thomas boundary conditions.¹ ϵ_n is taken identically zero over the entire depth l of the dead layer and the normal-incidence reflectance is evaluated using standard interference

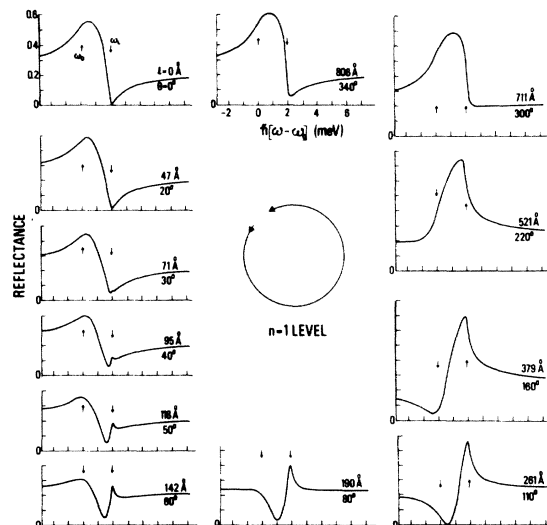


FIG. 5. Calculated line shape of the normal-incidence reflectance due to the $n=1$ level of the exciton. The interference dead-layer depth l (and the corresponding round-trip phase delay θ) is used as a parameter. The position of the transverse ω_0 and longitudinal ω_L exciton frequencies are shown by arrows.

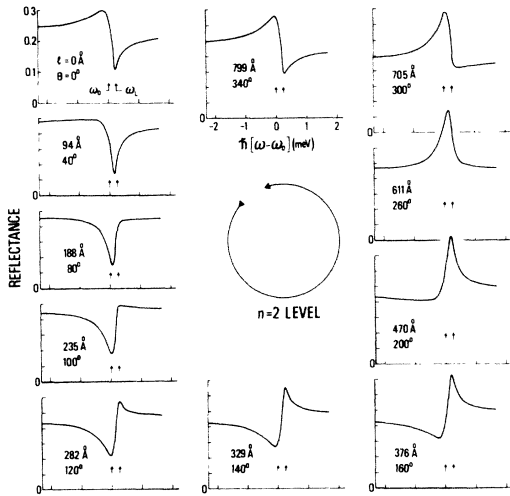


FIG. 6. Calculated line shape of the normal-incidence reflectance due to the $n=2$ level of the exciton. The interference dead-layer depth l (and the corresponding round-trip phase delay θ) is used as a parameter. The position of the transverse ω_0 and longitudinal ω_L exciton frequencies are shown by arrows.

formulas:

$$\tilde{r} = \frac{r_{12} + \tilde{r}_{23} e^{i\theta}}{1 + r_{12} \tilde{r}_{23} e^{i\theta}}, \quad (4)$$

$$\theta = 4\pi l / \lambda_m,$$

where $r_{12} = (1 - \sqrt{\epsilon_b}) / (1 + \sqrt{\epsilon_b})$ applies to the liquid-helium-dead-layer boundary and $\tilde{r}_{23} = (\sqrt{\epsilon_b} - \tilde{n}) /$

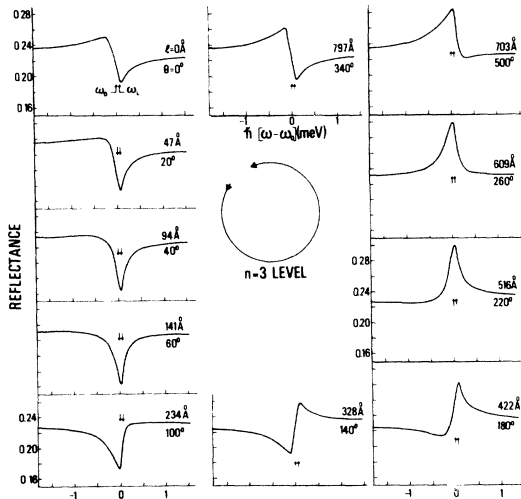


FIG. 7. Calculated line shape of the normal-incidence reflectance due to the $n=3$ level of the exciton. The interference dead-layer depth l (and the corresponding round-trip phase delay θ) is used as a parameter. The position of the transverse ω_0 and longitudinal ω_L exciton frequencies are shown by arrows.

$(\sqrt{\epsilon_b} + \tilde{n})$ to the dead-layer-bulk boundary. ϵ_b is the real background dielectric function and \tilde{n} is an effective complex refractive index¹ derived from the total K -dependent dielectric function $\tilde{\epsilon} = \epsilon_b + \tilde{\epsilon}_n$, with $\tilde{\epsilon}_n$ given by Eq. (3). Comparison with experiment will confirm *a posteriori* that this approximate model is surprisingly good at accounting for all the observed features of the reflectance spectra. The following parameters were used (Ref. 1): $4\pi\alpha = 0.0125$, $M^* = 0.9m_0$, $\hbar\omega_{01} = 2.5528$ eV, $\hbar\omega_{02} = 2.5759$ eV, $\hbar\omega_{03} = 2.5798$ eV, and $\epsilon_b = 8.1$. As to the broadening $\hbar\Gamma$, we have taken a value of 0.1 meV, capable of giving approximately the correct linewidth for all spectra and the appropriate ratio of the $n=1$ and $n=2$ amplitudes for sample 505/1 in Fig. 3.

Let us examine in detail the behavior of the calculated spectra in Figs. 5–7. The positions of the transverse (ω_0) and longitudinal (ω_L) exciton frequencies are indicated by the arrows. For all the three levels, recovery of the original line shape is achieved at 2π . A variety of shapes is seen in between; most noticeable is the region $l \approx 70$ – 150 Å for $n=1$, where a spike appears exactly at the longitudinal exciton frequency. For larger dead-layer depths the spike evolves towards a broad peak until over a π phase shift one observes an approximate reversal of the line shape. It should be mentioned that the evidence of the spike is conditioned by the choice of Γ , as illustrated for $l = 95$ Å in Fig. 8. Even for very small Γ , however, no spike appears in the $n=2$, $n=3$ structures, a consequence of the much weaker oscillator strength and transverse-longitudinal splitting. When the latter becomes comparable to the broadening, spatial dispersion effects are hardly of importance and the line shape resembles the classic one.

If we compare the calculated curves with the experimental spectra, it is immediately apparent that a different dead-layer depth applies to the various exciton levels. However, if the exciton-free layer were just of intrinsic origin, each exciton level would have a well-reproducible characteristic line shape. The as-grown surface must then present defects or surface states of the kind discussed in Sec. II (e.g., a Cd-rich region). The resulting surface field ionizes the exciton, in a manner which is more effective the weaker the binding energy of the level. One might question whether a built-in surface electric field can be sustained, at the low temperature of the experiment, in the presence of illumination. This has been discussed at some length in an earlier paper²⁴; it was concluded that, for low light-intensity levels, as in the present high-resolution experiments, the field is only slightly affected un-

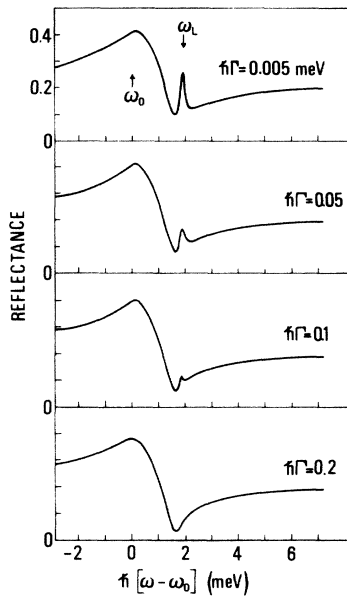


FIG. 8. Dependence on the broadening parameter $h\Gamma$ of one of the curves shown in Fig. 5.

less the generated carriers have a rather long recombination time. Of course, ionization by action of the surface field is not the only channel whereby surface defects can affect the exciton levels. Short surface lifetimes (as is in class II crystals) may also have some influence. We are not concerned with detailed mechanisms here, the only point we wish to make is that in general the intrinsic dead layer in CdS is somewhat altered by local conditions which vary from sample to sample. A look at the $n=1$ experimental spectra indicates that all line shapes are found approximately between $l \sim 70 \text{ \AA}$ and $l \sim 120 \text{ \AA}$, suggesting that the average exciton diameter [95 \AA as given by Eq. (2) for an effective Rydberg of 28 meV^1] is the dominant factor in setting the depth of the dead layer. However, the uneven behavior at frequency ω_L , the spike region, is due to the occasional presence of a few tens of angstroms of extrinsic origin. The situation for $n=2$ levels is quite different. Here the amplitude changes, rather than the line shape; this is because the extension of the intrinsic dead layer is large enough to be only weakly modified by extrinsic contributions, so that the round-trip phase θ is hardly affected. Note, on the other hand, that so far we have assumed a completely transparent dead layer, so that the light reflected at the deeper boundary crosses the layer twice without attenuation. This, in general, will not be true, because of absorption caused by surface defects and electric fields. For total absorption of the light in the round trip

through the dead layer, no indication of the exciton level will be found in the reflected intensity. For partial absorption, we expect a general reduction in the exciton features with respect to the background structureless reflectance. For any given surface condition, this should obviously be a more serious effect, the higher the exciton level considered. Quantitative inclusion of this effect in the calculated curves of Figs. 5-7 is trivial, and is omitted here for the sake of brevity.

From the above arguments, an important criterion can be established: The ideal case of a purely intrinsic dead layer can be approached by trying to maximize the amplitudes of the $n=2$ structures. In other words, one should take advantage of any possible treatment capable of attenuating the effect of the surface fields and/or damage. For instance, upon illumination with an auxiliary source of white light, we noted a variation, either up or down, of the magnitude of the spike in the $n=1$ region and an increase in amplitude of the $n=2$ structure. This type of random illumination dependence of the spike has been observed also by Broser²⁵ and other related effects are discussed by Permogorov *et al.*²⁶; therefore we shall not further analyze this behavior. A second manner of controlling the surface behavior is to apply external fields. The results of this work will be reported separately. We shall concentrate here on the technique of heat treatments, which can alter the surface extrinsic dead layer, as anticipated in Sec. II. We have seen that the spectral behavior of our as-grown crystal fits well in the Cd-rich layer description for class I CdS. A moderate treatment should result in evaporation of the excess cadmium and probable cancellation of the electric field, as there are very little oxygen states left after preevacuation of the liquid-helium chamber. Various heat treatments in vacuum have been attempted. The second curve from top in Fig. 3 illustrates a case when the amplitude of the $n=2$ structure is strongly enhanced with respect to the virgin sample (top curve) and a $n=3$ structure develops in form of a dip (see also magnified detail). The temperature cycling was as follows: The sample was heated in a 2×10^{-6} Torr vacuum from room temperature up to 790°C in 2 min, then baked at 790°C for 2 min and finally cooled rapidly. After this treatment, the sample was transferred to the cryostat and the standard cooling procedure was followed. We believe that the resulting spectrum is very close to the virtually ideal spectral line shape, and corresponds to the loss of the excess Cd donors in the surface layer. In no other instance were we able to get such clear evidence of the $n=2$ and $n=3$ excited states. In

addition, these levels were only weakly affected in this case by illumination with white light. We proceed then to compare this spectrum with the calculated curves of Figs. 5–7. Here again, comparison can only be qualitative, in particular for the excited levels, because the theory neglects absorption in the dead layer. The parameters determined are listed in Table I. In view of the rather drastic approximations made in the calculations and of the relatively coarse correlation between the exciton average size and the actual region of optical interference, the results are unexpectedly good and provide a substantial support to the physical model invoked. To give our results more generality, let us examine the reflectance spectra of other materials available in the literature and try to fit their behavior within the general ideas discussed in this paper. To do this, we should recalculate the curves of Figs. 5–7 with appropriate changes of the important parameters, i.e., $4\pi\alpha$, M^* , and Γ . This could be done, but it goes far beyond the objectives of the present work. We know, however, that the main qualitative features illustrated in Figs. 5–7 do not change appreciably, within factors of 5 or so in the said parameters. For instance, we know from a best-fit procedure that in GaAs, where only $n=1$ is detected, the dead layer is 260 \AA ($\theta=91^\circ$).¹⁰ Perusal of Fig. 5 gives $\theta=80^\circ$ (although $4\pi\alpha$ in GaAs is as much as eight times smaller) and Fig. 6 gives $\theta=90^\circ$. The same conclusion is obtained from a consideration of InP.¹⁰ For semiconductors with gap in the visible or near infrared and spectra taken near liquid-helium temperature, we can therefore rely well on the present calculations to get a feeling about many materials. Consideration of the curves shown here and of other sets for different Γ , leads to Table II, giving approximate dead-layer depth, interference angles, and average exciton sizes for a number of cases considered.

The results of Tables I and II confirm that there is a steady correspondence between the dead-layer depth and the exciton size, although the latter is always larger by a factor of about 1.5. It should be remarked that the type of line-shape analysis

which we have presented here can be useful as a means of surface diagnostics and also as a supporting experimental approach for the determination of the effective Bohr radius of the exciton.

B. Heavily treated crystals

Further confirmation of the validity of our approach, and in particular, of the picture in terms of the dead-layer boundary condition by Hopfield and Thomas with spatial dispersion, comes from the consideration of what we call heavily treated crystals. By this we mean crystals where the reflectance line shape, rather than approaching the ideal intrinsic dead-layer limit, evolves toward a behavior which is described by larger values of the phase delay in Figs. 5–7. Two typical experimental spectra are shown in Fig. 3. The third curve from top (505/2), was obtained by further heating sample 505 to 940°C , following the same procedure described above. It is apparent that a heavily damaged surface layer has developed. The drastic modification of the line shape points to a dead layer of $\sim 190 \text{ \AA}$ (see curve 7 counterclockwise in Fig. 5). As a consequence of the increased absorption, the B exciton appears rather weaker than the A exciton and the $n=2$ level disappears. Similar results are obtained by heating in an inert atmosphere (helium). Cycling as before up to 800°C gave rise to the bottom curve in Fig. 3 (sample 514). The dead layer here corresponds to about 500 \AA (note, however, that in both this case and the previous one, one cannot rule out in principle a possible additional $2\pi N$ phase shift). The process which is likely to occur during heat treatments is simultaneous evaporation of Cd and S,¹⁹ in different amounts, so as to regenerate a heavily doped surface layer. The shortness of the treatment should not allow appreciable diffusion and prevents homogenization of the sample. From our results it is therefore clear that surface states or defects are very important in determining even the gross features of exciton reflectance spectra. We have taken a few extreme cases of heavy damage, but it is possible to envisage more

TABLE I. Dead-layer depth and phase delay for the three lowest levels of the A exciton of CdS, as estimated from comparison of observed and calculated line shapes. The average exciton size is obtained from Eq. (2).

CdS	Dead-layer depth (\AA)	Average exciton size (\AA)	Phase delay (deg)
$n=1$	~ 70	95	~ 30
$n=2$	~ 300	380	~ 130
$n=3$	~ 980	850	~ 420

TABLE II. Dead-layer depth, phase delay, and exciton average size for semiconductors other than CdS.

Material	Level	Dead-layer depth (Å)	Average exciton size (Å)	Phase delay (deg)
GaAs ^a	1	295	405	91
InP ^a	1	260	365	80
ZnSe ^b	1	~ 75	126	~ 35
	2	~ 300	504	~ 130
CdSe ^c	1	~ 152	162	~ 53
ZnTe ^d	1	~ 138	210	~ 57

^aReference 10.

^bReference 20.

^cReference 21.

^dReference 1.

sophisticated and careful surface treatments to follow the evolution of the spectra through all the calculated line shapes in better detail. A parallel experiment could be to apply external fields, as was done earlier for the III-V's.^{10,23}

The possibility of varying the dead-layer depth provides us with an useful degree of freedom in view of ruling out alternative explanations to our results. We know that simple interference theory without spatial dispersion gives unreasonably large values of the reflectance unless huge dampings and unrealistically low oscillator strengths are used. In no case, however, does it succeed in producing a spike at $\omega = \omega_L$ for $n=1$ (an example of this can be found in Fig. 9). There is a

feature, however, which could cast some doubts on the unicity of the Hopfield and Thomas dead-layer model as a possible source for the spike. The exciton in CdS should be split into a doublet²⁷ because of the bimolecular nature of the unit cell. Evidence of this splitting has been claimed in some transmission measurements,²⁸ where an extra peak is observed at the longitudinal exciton frequency. The reflectance spike would then be a volume rather than a surface effect. With this in mind, we have calculated the normal-incidence reflectance, using classical interference formulas, for a pair of oscillators, split by 2 meV (i.e., approximately the transverse-longitudinal splitting). If for the upper level of the doublet one takes a much lower oscillator strength, it is indeed possible to generate a spike at $\omega = \omega_L$. We shall demonstrate, however, that this result is rather accidental, as it seems to fit only the limit of small dead-layer depth, while failing to account for the data obtained in heavily treated samples. The results of our calculation are shown in Fig. 9 (solid lines). We have taken $\hbar\Gamma = 0.2$ meV, $4\pi\alpha_1 = 0.0125$ (i.e., the same as for the spatial dispersion case of Fig. 5), and $\alpha_2 = 10^{-2}\alpha_1$. The round-trip phase delay θ was parametrically varied exactly as done in Fig. 5. For comparison, the behavior due to the lower oscillator alone is shown by the dashed curves: It is seen that the only effect of the weaker split-off exciton is to dig a hole in the main contribution from the lower level. Consideration of the two-oscillator spectra allows the following conclusions to be drawn. Apart from the over-all quantitative disagreement with experiment as to general line shape and reflectance amplitude, it is apparent that in the region for l between 0 and ~ 140 Å an extra peak, resembling the experimental spike at $\omega = \omega_L$, is present. However, for large dead-layer depths, the dip associated to the split off exciton is never washed out,

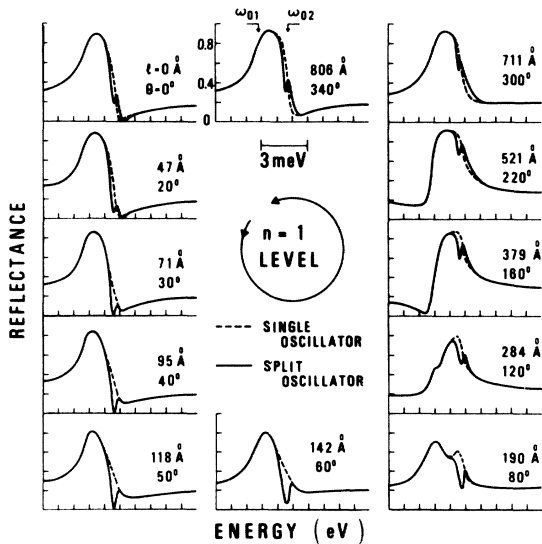


FIG. 9. Calculated normal-incidence for the $n=1$ level in absence of spatial dispersion. Dashed curves for single oscillator; solid curves for split oscillator (see text for details). The dead-layer depth l is used as a parameter.

in sharp contrast with the experimental results of Fig. 3. It is obvious that, if the two components of the exciton doublet were taken of comparable strength, as suggested in Ref. 28, the discrepancy with experiment would be even worse. We conclude therefore that the heavily treated samples support the view that a single oscillator with spatial dispersion is quite adequate at uniquely explaining all our results.

IV. SUMMARY AND CONCLUSIONS

By analyzing the normal-incidence reflectance structures of the *A* exciton in CdS, we have clearly established that an important size effect has direct influence on the line shapes. A surface dead layer, i.e., an inhomogeneous region where the exciton concentration is virtually zero, gives rise to optical-interference effects which are strictly dependent on the particular material and exciton level considered. Experiments on virgin and heat-treated crystals indicate that surface fields and damage play some role in altering the depth of this layer from crystal to crystal. Even in the case of an ideal surface, however, the dead layer is present as an intrinsic feature related to the finite size of the exciton. This has been confirmed

by looking at the first three levels of the excitonic series, whose line-shape behavior has shown one-to-one correlation with the value of the corresponding effective Bohr radii. An analysis of the results previously known from the literature for other II-VI and III-V semiconductors indicates that the picture we have drawn for CdS has a more general significance. The conclusions of this work give valid support to the spatial dispersion picture by Hopfield and Thomas and to the related additional boundary conditions, while discouraging interpretation of the spike at the longitudinal exciton frequency in terms of an exciton splitting.

ACKNOWLEDGMENTS

The authors are very grateful to Dr. W. A. Albers, Jr. and Dr. D. M. Roessler for kindly supplying a number of samples. For the same reason, and for making his latest results known prior to publication, the authors feel very indebted to Professor K. W. Boer. Thanks are due to R. Generosi and S. Rinaldi for technical assistance during the experiment and to Professor G. Chiarotti for useful discussion and encouragement.

*Also at: Istituto di Matematica, Università di Camerino, Italy.

†Gruppo Nazionale di Struttura della Materia del C.N.R.

¹J. J. Hopfield and D. G. Thomas, *Phys. Rev.* **132**, 563 (1963).

²S. I. Pekar, *Zh. Eksp. Teor. Fiz.* **33**, 1022 (1957) [*Sov. Phys.—JETP* **6**, 785 (1958)]; **34**, 1176 (1958) [**7**, 813 (1958)].

³V. M. Agranovich and V. L. Ginzburg, *Spatial Dispersion in Crystal Optics and the Theory of Excitons* (Wiley, New York, 1967).

⁴G. S. Agarwal, D. N. Pattanayak, and E. Wolf, *Phys. Rev. Lett.* **27**, 1022 (1971); *Optics Commun.* **4**, 255; **4**, 260 (1971).

⁵T. Skettrup and I. Balslev, *Phys. Rev. B* **3**, 1457 (1971).

⁶J. J. Sein, *J. Opt. Soc. Am.* **62**, 1037 (1972).

⁷J. Biellman, M. Grossman, and S. Nikitine, *Polaritons* (Pergamon, New York, 1974).

⁸D. D. Sell, R. Dingle, S. E. Stokowski, and J. V. DiLorenzo, *Phys. Rev. B* **7**, 4568 (1973).

⁹I. Filinski and T. Skettrup, *Solid State Commun.* **11**, 1651 (1972).

¹⁰F. Evangelisti, J. U. Fischbach, and A. Frova, *Phys. Rev. B* **9**, 1516 (1974).

¹¹E. F. Gross and B. V. Novikov, *Fiz. Tverd. Tela.* **1**, 1882 (1959) [*Sov. Phys.—Solid State* **1**, 1723 (1960)].

¹²P. Mark, *J. Phys. Chem. Solids* **25**, 1911 (1964); C. E. Reed and C. G. Scott, *Br. J. Appl. Phys.* **15**, 1045 (1964).

¹³C. E. Bleil and W. A. Albers, Jr., *Surf. Sci.* **2**, 307 (1964).

¹⁴C. L. Balestra, J. Lagowski, and H. C. Gatos, *Surf.*

Sci. **26**, 317 (1971); F. Steinrisser and R. E. Hetrick, *Surf. Sci.* **28**, 607 (1971).

¹⁵E. F. Gross and B. V. Novikov, *J. Phys. Chem. Solids* **22**, 87 (1961).

¹⁶E. H. Weber, *Phys. Status Solidi* **28**, 649 (1968).

¹⁷K. Colbow, A. Jmaeff, and K. Yuen, *Can. J. Phys.* **48**, 57 (1970).

¹⁸R. Schubert and K. W. Boer, *J. Phys. Chem. Solids* **32**, 77 (1971).

¹⁹J. A. Bragagnolo, C. Wright, and K. W. Boer (unpublished); J. A. Bragagnolo and K. W. Boer (unpublished).

²⁰G. E. Hite, D. T. F. Marple, M. Aven, and B. Segall, *Phys. Rev.* **156**, 850 (1967).

²¹R. G. Wheeler and J. O. Dimmock, *Phys. Rev.* **125**, 1805 (1962).

²²M. F. Deigen and M. D. Glinchuk, *Fiz. Tverd. Tela.* **6**, 3250 (1963) [*Sov. Phys.—Solid State* **5**, 2377 (1964)].

²³F. Evangelisti, A. Frova, and J. U. Fischbach, *Phys. Rev. Lett.* **29**, 1001 (1972).

²⁴A. Frova, F. Evangelisti, and M. Zanini, *Phys. Status Solidi A* **24**, 315 (1974).

²⁵I. Broser (private communication).

²⁶S. A. Permogorov, V. V. Travnikov, and A. V. Sel'kin, *Fiz. Tverd. Tela.* **14**, 3642 (1972) [*Sov. Phys.—Solid State* **14**, 3051 (1973)].

²⁷S. A. Moskalenko and M. I. Shmiglyuk, *Fiz. Tverd. Tela.* **6**, 3535 (1964) [*Sov. Phys.—Solid State* **6**, 2831 (1965)].

²⁸M. S. Brodin, A. V. Kritskii and M. I. Strashnikova, *Zh. Eksp. Teor. Fiz. Pis'ma Red.* **10**, 217 (1969) [*JETP Lett.* **10**, 136 (1969)].